Journal of Coordination Chemistry

ISSN: 0095-8972 (Print) 1029-0389 (Online) Journal homepage: http://www.tandfonline.com/loi/gcoo20

Coordination chemistry of 2,6-dimethanol pyridine with early transition metal alkoxide compounds

Timothy J. Boyle, Michael L. Neville, Daniel T. Yonemoto, Todd M. Alam & Lily Jan

To cite this article: Timothy J. Boyle, Michael L. Neville, Daniel T. Yonemoto, Todd M. Alam & Lily Jan (2015) Coordination chemistry of 2,6-dimethanol pyridine with early transition metal alkoxide compounds, Journal of Coordination Chemistry, 68:9, 1616-1632, DOI: 10.1080/00958972.2015.1028382

To link to this article: http://dx.doi.org/10.1080/00958972.2015.1028382

Accepted author version posted online: 19 Mar 2015.
Published online: 09 Apr 2015.

Journal of Coordination Chemistry, 2015
Vol. 68, No. 9, 1616–1632, http://dx.doi.org/10.1080/00958972.2015.1028382

Coordination chemistry of 2,6-dimethanol pyridine with early transition metal alkoxide compounds

TIMOTHY J. BOYLE*, MICHAEL L. NEVILLE, DANIEL T. YONEMOTO, TODD M. ALAM and LILY JAN

Advanced Materials Laboratory, Sandia National Laboratories, Albuquerque, NM, USA

(*Received 5 January 2015; accepted 24 February 2015*)

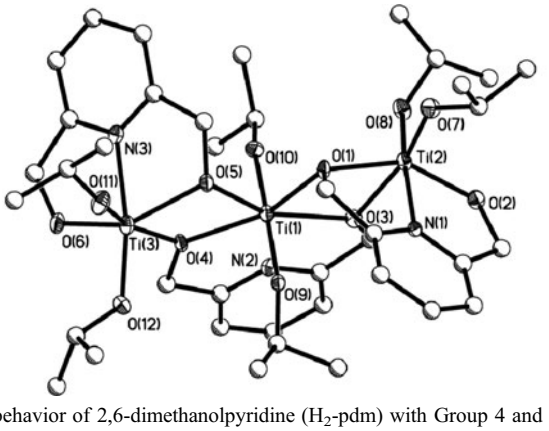

The coordination behavior of 2,6-dimethanolpyridine (H_2-pdm) with Group 4 and 5 metal alkoxides was crystallographically determined. The pdm ligand was found to undergo a variety of tridentate, bridging coordination configurations: $(OR)_2M(\mu^2\text{–pdm})[(\mu\text{–pdm})M(OR)_2]_2$ (*shown*), $M_3(\mu^3\text{–pdm})(\mu\text{–pdm})_2(OR)_6$, or $[M(\mu\text{–pdm})(OR)_3]_2$.

The coordination behavior of the 2,6-dimethanol pyridine (H_2-pdm) with Group 4 and 5 metal alkoxides was undertaken through a series of alcoholysis reactions. The products were crystallographically identified as: $(OR)_2M(\mu^2\text{-pdm})[(\mu\text{-pdm})M(OR)_2]_2$ (M = Ti, OR = OPr^i (**1** · py), ONep (**2** · HONep, tol); Zr, OBu^t (**3**)), $[M_3(\mu^3\text{-pdm})(\mu\text{-pdm})_2(\mu\text{-ONep})_2(ONep)_4]$ (M = Zr (**4**), Hf (**5**)), $[M(\mu\text{-pdm})(OR)_3]_2$ [M/OR = Nb/OEt (**6**), and Ta/ONep (**7**)] where $\mu = \eta^1,\eta^1,\eta^2(O,N,O')$, $\mu^2 = \eta^2,\eta^1,\eta^2(O,N,O')$, $\mu^3 = \eta^1,\eta^1,\eta^3(O,N,O')$, OEt = OCH_2CH_3, OPr^i = $OCH(CH_3)_2$, OBu^t = $OC(CH_3)_3$, and ONep = $OCH_2C(CH_3)_3$. For each complex, pdm was a bichelating (O,N,O′) ligand generating trinuclear species coupled with a variety of additional bridging modes: μ, μ^2, and μ^3. Further analyses by multinuclear and DOSY NMR studies indicated that the structures were retained in solution.

Keywords: Alkoxides; Pyridine; Group 4; Titanium; Zirconium; Hafnium

*Corresponding author. Email: tjboyle@Sandia.gov

1. Introduction

Control over the final structure of metal alkoxides ([$M(OR)_4$]) for the production of tailored ceramic oxide materials is of continued interest. Attempts to realize this goal have been widely investigated through the use of chelating ligands [1–10]. The polydentate nature of these ligands will influence the structure of metal alkoxides by filling open coordination sites while minimally consuming the metal's available charge [1–12]. Following this thematic approach, we previously reported the impact that a set of bidentate alkoxide ligands [i.e. thiophene methanol (SC_4H_3-(CH_2OH)-2), tetrahydrofuran methanol (OC_4H_7(CH_2OH)-2), or pyridine carbinol ((NC_5H_4(CH_2OH)-2) or H-OPy)] [11, 12] had on the final structural properties of [$M(OR)_4$]. Of this set of modifiers, the bidentate H-OPy [figure 1(a)] ligand was also found to impart control over both the structure isolated and over other alcoholysis chemical modifications. For the Group 4 modified products, the *bis*-OPy chelating arrangement was stable and allowed for controlled substitution of the parent alkoxide without disrupting the monomeric arrangement [11, 12].

Due to the success with the OPy ligand, further exploration of pyridine-alcohol-like modifying ligands was warranted. One of the ligands investigated was the 2,6-di-methanol pyridine [H_2-pdm, figure 1(b)] which can adopt a number of coordination geometries [figure 1(c)–(f)]. However, a search of the literature concerning the coordination behavior of pdm with early transition metals revealed, surprisingly little structural information [1]. Of the reported structures, the majority of pdm-modified compounds were found to employ a chelating mode [η^1, η^1, η^1 (O,N,O); figure 1(c)] for this ligand [13–21]. Due to this void, we undertook a detailed study of the products formed from the reaction of this ligand with a series of early transition [$M(OR)_x$] from Group 4 [equation (1); $x = 4$] and 5 [equation (1); $x = 5$]. The products from equation (1) were crystallographically identified as $(OR)_2M(\mu^2\text{-pdm})[(\mu\text{-pdm})M(OR)_2]_2$ (M = Ti, OR = OPr^i (**1** · py), ONep (**2** · HONep, tol); Zr/OBu^t (**3**)), $[M_3(\mu^3\text{-pdm})(\mu\text{-pdm})_2(\mu\text{-ONep})_2(ONep)_3]$ (M = Zr (**4**), Hf (**5**)), $[M(\mu\text{-pdm})(OR)_3]_2$ [M/OR = Nb/OEt (**6**), and Ta/ONep (**7**)], where $\mu = \eta^1,\eta^1,\eta^2$(O,N,O′), $\mu^2 = \eta^2,\eta^1,\eta^2$(O,N, O′), $\mu^3 = \eta^1,\eta^1,\eta^3$(O,N,O′), OEt = OCH_2CH_3, OPr^i = $OCH(CH_3)_2$, OBu^t = $OC(CH_3)_3$, and ONep = $OCH_2C(CH_3)_3$. Bonding modes observed above are shown in figure 1(d)–(f). The synthesis and characterization of these compounds are discussed in detail.

$$[M(OR)_x] + H_2\text{-pdm} \longrightarrow (OR)_{x-2}M(pdm) + 2HOR \quad (1)$$

2. Experimental section

All compounds described below were handled with rigorous exclusion of air and water using standard Schlenk line and glove box techniques. All solvents were used as received (Aldrich) in Sure/Seal™ bottles and stored under argon, including toluene (tol), tetrahydrofuran (THF), and pyridine (py). The following chemicals were used as received (Aldrich) and stored under argon: H_2-pdm, [$M(OBu^t)_4$] (M = Ti, Zr, Hf). The $[Ti(ONep)_4]_2$ [22], $[M_2(\mu\text{-ONep})_3(ONep)_6(HOBu^t)]$ (M = Zr, Hf; $[M(ONep)_4]$) [23], and $[M(\mu\text{-OEt})(ONep)_4]_2$ (M = Nb, Ta; [M(ONet)]) [24] compounds were synthesized according to the published results.

FTIR spectral data were obtained on a Nicolet 6700 FTIR spectrometer using KBr pellets pressed under an argon atmosphere and handled under an atmosphere of flowing nitrogen. Elemental analyses were performed on a Perkin Elmer 2400 CHN-S/O elemental analyzer.

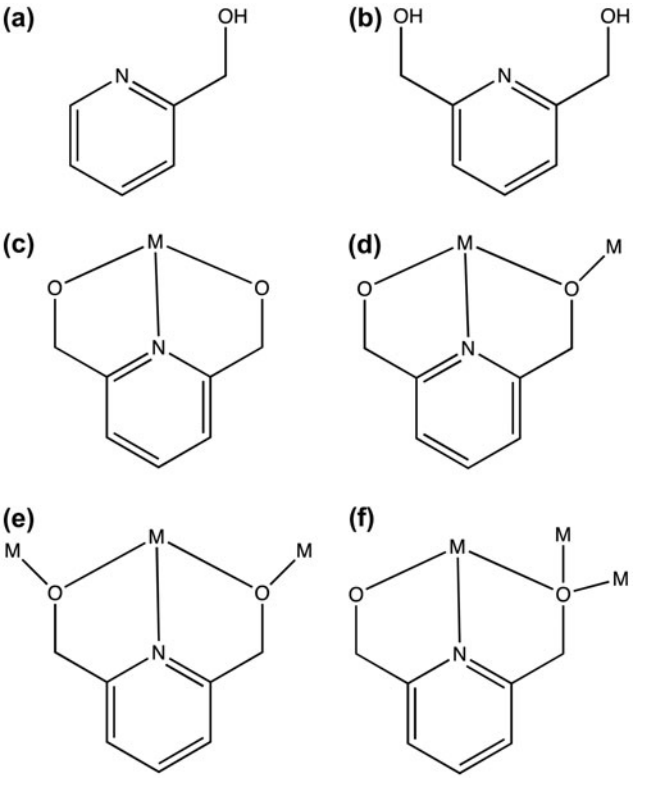

Figure 1. Schematic representation of (a) H-OPy and (b) H_2-pdm and the observed bonding modes of the pdm ligand, (c) chelating = η^1, η^1, η^1 (O,N,O′), (d) $\mu = \eta^1$, η^1, η^2 (O,N,O′), (e) $\mu^2 = \eta^2$, η^1, η^2 (O,N,O′), (f) $\mu^3 = \eta^1$, η^1, η^3 (O,N,O′).

All NMR samples were prepared by dissolving crystalline material in the appropriate deuterated solvent followed by flame sealing under vacuum. All NMR spectra were obtained on a Bruker Avance III 500 under standard experimental pulse field gradient (PFG) conditions. A bipolar stimulated echo was used for all experiments.

2.1. *General synthesis*

To a stirring solution of the desired $[M(OR)_4]$ dissolved in tol, stoichiometric amounts of H_2-pdm were added. The solution immediately turned a pale shade of yellow and was stirred for 12 h. If a precipitate was formed, THF and/or pyridine was added to the mixture and low heat was applied. Once the sample dissolved completely, the reaction mixture was set-aside until X-ray quality crystals were formed. For the non-heated samples, the crystals were formed by slow evaporation. Yields were not optimized but reflect the first batch of crystals isolated. Crystals were put aside for single-crystal X-ray experiments and dried crystals were used for all additional analyses.

2.1.1. $(OPr^i)_2Ti(\mu^2\text{–pdm})[(\mu\text{–pdm})Ti(OPr^i)_2]_2$ (1) · py. Used $[Ti(OPr^i)_4]$ (0.500 g, 1.76 mmol), H_2-pdm (0.244 g, 1.76 mmol) in ~2 mL of hexanes and ~3 mL of py. Yield

21.6% (0.115 g). FTIR (KBr, cm^{-1}) 3068 (w), 2963 (m), 2925 (m), 2856 (m), 2826 (m), 2611 (w), 1602 (s), 1581 (s), 1470 (s), 1439 (m), 1413 (w), 1401 (w), 1369 (w), 1356 (m), 1332 (m), 1265 (w), 1216 (w), 1160 (s), 1108 (s), 1070 (s), 1030 (s), 995 (s), 953 (w), 845 (m), 787 (m), 731 (w), 696 (w), 656 (m), 554 (m), 464 (w), 454 (w), 438 (w, sh). ^{1}H NMR (500.1 MHz, $CDCl_3$) δ 7.85 (2H, t, $NC_5H_3(CH_2O)_2$), 7.27 (3.8H, mult, $NC_5H_3(CH_2O)_2$), 5.82 (5.1H, s, $NC_5H_3(CH_2O)_2$), 5.69 (3.6H, s, $NC_5H_3(CH_2O)_2$), 4.73 (0.9H, sept, $OCH(CH_3)_2$, $J_{H\text{-}H}$ = 5 Hz), 4.48 (1.3H, sept, $OCH(CH_3)_2$, $J_{H\text{-}H}$ = 5 Hz), 1.20 (18H, mult., $OCH(CH_3)_2$). Anal. Calcd for $C_{44}H_{68}N_4O_{12}Ti_3$ (%): C, 53.46; H, 6.93; N, 5.67. Found: C, 53.06; H, 7.57; N, 4.93.

2.1.2. $(ONep)_2Ti(\mu^2\text{–pdm})[(\mu\text{–pdm})Ti(ONep)_2]_2$ (2) · HONep, tol. Used $[Ti(ONep)_4]$ (0.500 g, 1.26 mmol), H_2-pdm (0.176 g, 1.26 mmol) in ~2 mL of tol. Yield 23.6% (0.107 g). FTIR (KBr, cm^{-1}) 2950 (s), 2901 (m), 2864 (s), 2825 (m), 2685 (w), 1603 (m), 1583 (m), 1472 (s), 1448 (w, sh), 1439 (m), 1390 (w), 1359 (m), 1340 (w), 1263 (m), 1216 (w), 1157 (m), 1091 (s, sh), 1070 (s), 1023 (s), 934 (w), 900 (w), 790 (m), 751 (w), 729 (w), 724 (w, sh), 675 (s, sh), 669 (s), 555 (w), 535 (w), 472 (m), 469 (m), 459 (w, sh). ^{1}H NMR (500.1 MHz, $CDCl_3$) δ 7.79 (2H, mult, $NC_5H_3(CH_2O)_2$), 7.22 (4H, mult., $NC_5H_3(CH_2O)_2$), 5.76 (5.6H, s, $NC_5H_3(CH_2O)_2$), 5.66 (3.2H, s, $NC_5H_3(CH_2O)_2$), 3.93 (5.9H, mult (br), $OCH_2C(CH_3)_3$), 0.82 (41H, s, $OCH_2C(CH_3)_3$). Anal. Calcd for $C_{17}H_{29}NO_4Ti$ (%): C, 56.83; H, 8.14; N, 3.90. Found: C, 56.85; H, 8.53; N, 3.52.

2.1.3. $(OBu^t)_2Zr(\mu^2\text{–pdm})[(\mu\text{–pdm})Zr(OBu^t)_2]_2$ (3). Used $[Zr(OBu^t)_4]$ (0.500 g, 1.30 mmol), H_2-pdm (0.181 g, 1.30 mmol) in ~2 mL of tol and ~3 mL of py. Yield 48.8% (0.238 g). FTIR (KBr, cm^{-1}) 2965 (s), 2937 (m), 2921 (m), 2897 (m), 2861 (m), 2822 (w), 1605 (s), 1581 (s), 1468 (s), 1450 (m), 1439 (m), 1422 (w), 1377 (s), 1354 (s), 1260 (m), 1225 (s), 1209 (s), 1198 (s, sh), 1159 (m), 1108 (s), 1074 (s), 1052 (s), 1023 (s), 1009 (s, sh), 907 (w), 777 (s), 748 (w), 672 (m), 654 (m), 635 (m), 538 (w, sh), 527 (m), 511 (s, sh), 477 (m), 445 (m), 405 (s). ^{1}H NMR (500.1 MHz, $CDCl_3$) δ 7.79 (2H, t, $NC_5H_3(CH_2O)_2$), 7.22 (3.8H, mult, $NC_5H_3(CH_2O)_2$), 5.76 (5.1H, s, $NC_5H_3(CH_2O)_2$), 5.61 (2.5H, s, $NC_5H_3(CH_2O)_2$), 1.20 (15.1H, mult., $OCH(CH_3)_2$), 0.91 (9.4H, s, $OCH(CH_3)_2$). Anal. Calcd for $C_{65}H_{105}N_5O_{16}Zr_4$ (%; **3** + py): C, 49.49; H, 6.71; N, 4.44. Found: C, 49.41; H, 6.74; N, 4.56.

2.1.4. $Zr_3(\mu^3\text{–pdm})(\mu\text{–pdm})_2(ONep)_6$ (4). Used $[Zr(ONep)_4]$ (0.500 g, 1 mmol), H_2-pdm (0.146 g, 1.13 mmol) in ~2 mL of tol and ~ 2 mL of THF. Yield 27.7% (0.117 g). FTIR (KBr, cm^{-1}) 3070 (w), 2949 (s), 2904 (m), 2863 (s), 2819 (m), 2742 (w), 2696 (w), 1973 (w), 1607 (s), 1581 (s), 1478 (s, sh), 1468 (s), 1452 (m), 1441 (m), 1392 (m), 1359 (s), 1346 (m, sh), 1294 (w), 1259 (w), 1214 (w), 1159 (s), 1113 (s), 1071 (s), 1044 (s), 1023 (s), 934 (w), 918 (w), 900 (w), 833 (w), 776 (s), 749 (w), 729 (w), 657 (m, sh), 636 (s), 589 (w), 575 (w), 532 (w), 508 (w), 485 (m), 454 (s). Anal. Calcd for $C_{55}H_{95}N_3O_{13}Zr_3$ (%; **3** + THF): C, 51.61; H, 7.48; N, 3.28. Found: C, 51.38; H, 7.84; N, 3.36.

2.1.5. $Hf_3(\mu^3\text{–pdm})(\mu\text{–pdm})_2(ONep)_6$ (5). Used $[Hf(ONep)_4]$ (0.500 g, 0.948 mmol), H_2-pdm (0.132 g, 0.948 mmol) in ~2 mL of THF, ~3 mL of py. Yield 21.8% (0.0946 g). FTIR (KBr, cm^{-1}) 3449 (m, sh), 3423 (m), 3414 (m, sh), 3186 (w), 2950 (s), 2408 (m, sh),

2864 (m), 2837 (m, sh), 2824 (m, sh), 2388 (w), 2347 (w), 1618 (w, sh), 1609 (m), 1583 (m), 1478 (m), 1467 (m), 1461 (m, sh), 1443 (m), 1392 (w), 1359 (m), 1261 (m), 1214 (w), 1175 (m, sh), 1160 (m), 1113 (s), 1070 (s), 1045 (s), 1022 (s), 801 (m), 778 (m), 659 627 (m), 591 (w), 509 (w, sh), 503 (w, sh), 478 (m, sh), 468 (m, sh), 455 (m), 446 (m). Anal. Calcd for $C_{56}H_{92}Hf_3N_4O_{12}$ (%; **5** + py): C, 43.43; H, 5.99; N, 3.62. Found: C, 44.01; H, 5.94; N, 3.89.

2.1.6. [Nb(μ–pdm)(OEt)$_3$]$_2$ (6). Used [Nb(ONet)$_5$] (0.500 g, 1.57 mmol), H_2-pdm (0.219 g, 1.57 mmol) in ~2 mL of tol. Yield 69.0% (0.396 g). FTIR (KBr, cm^{-1}) 3083 (w), 3072 (w), 3056 (w), 3044 (w), 3017 (w), 2963 (w), 2921 (w), 2885 (w), 2844 (w), 2733 (w), 2691 (w), 1608 (m), 1581 (w), 1470 (m), 1459 (w), 1439 (w), 1372 (m), 1351 (m), 1263 (w), 1220 (w), 1159 (s, sh), 1139 (s), 1107 (s), 1059 (s), 1027 (s, sh), 912 (s), 796 (m), 786 (m, sh) 758 (w), 727 (w), 674 643 (w), 579 534 (w), 512 (w), 485 (m), 459 (w), 428 (w). ^{1}H NMR (500.1 MHz, $CDCl_3$) δ 7.80 (2H, t, $NC_5H_3(CH_2O)_2$), 7.15 (4H, d, $NC_5H_3(CH_2O)_2$), 5.80 (8H, s, $NC_5H_3(CH_2O)_2$), 4.58 (3H, s(br), $NC_5H_3(CH_2O)_2$), 3.98 (7.6H, s(br) OCH_2CH_3), 1.33 (6.5H, s, OCH_2CH_3), 0.83 (10H, s(br), OCH_2CH_3). Anal. Calcd for $C_{13}H_{22}NNbO_5$ (%): C, 42.75; H, 6.07; N, 3.84. Found: C, 42.09; H, 6.00; N, 3.86.

2.1.7. [Ta(μ–pdm)(ONep)$_3$]$_2$ (7). Used [Ta(ONet)$_5$] (0.500 g, 1.23 mmol), H_2-pdm (0.171 g, 1.23 mmol) in ~2 mL of tol. Yield 69.0% (0.396 g). FTIR (KBr, cm^{-1}) 2948 (s), 2899 (s), 2863 (s), 2835 (s), 2698 (m), 1612 (m), 1584 (w), 1474 (m), 1474 (m), 1461 (w, sh), 1441 (w), 1390 (m), 1355 (m), 1258 (w), 1222 (w), 1153 (m, sh), 1102 (s), 1069 (s), 1024 (s), 830 (w), 796 (w), 780 (m), 751 (w), 730 (w), 683 (m, sh), 647 (s), 50 l (m, sh), 487 (s), 452 (m), 429 (w), 406 (w). ^{1}H NMR (500.1 MHz, $CDCl_3$) δ 7.80 (1H, t, $NC_5H_3(CH_2O)_2$), 7.74 (1.1H, t, $NC_5H_3(CH_2O)_2$), 7.13 (4.2H, mult., $NC_5H_3(CH_2O)_2$), 5.85 (7.5H, s, $NC_5H_3(CH_2O)_2$), 3.56 (4.8H, s, $OCH_2C(CH_3)_3$), 0.72–0.47 (52H (mult)s, $OCH_2C(CH_3)_3$). Anal. Calcd for $C_{44}H_{80}N_2O_{10}Ta_2$ (%): C, 45.60; H, 6.96; N, 2.42; $C_{19}H_{34}NO_5Ta$ (%; **7** – 3 CH_3): C, 42.46; H, 6.38; N, 2.61. Found: C, 42.71 H, 6.37 N 2.67.

2.2. *General X-ray crystal structure information*

Single-crystals were mounted onto a loop from a pool of Paratone™ oil and immediately placed in a cold N_2 vapor stream, on a Bruker AXS diffractometer employing an incident-beam graphite monochromator, MoKa radiation (λ = 0.71070 Å) and a SMART APEX CCD detector. Lattice determination and data collection were carried out using SMART Version 5.054 software. Data reduction was performed using SAINTPLUS Version 6.01 software and corrected for absorption using the SADABS program within the SAINT software package. Structures were solved by direct methods or by using the PATTERSON method that yielded the heavy atoms, along with a number of the lighter atoms. Subsequent Fourier syntheses yielded the remaining light-atom positions. Hydrogens were fixed in positions of ideal geometry and refined using SHELX software. The final refinement of each compound included anisotropic thermal parameters for all non-hydrogen atoms. All final CIF files were checked using the CheckCIF program (http://www.iucr.org/). Additional information concerning data collection and final structural solutions can be found by accessing CIF files through the Cambridge Crystallographic Data Base. Table 1 lists the unit cell parameters for the structurally characterized **1**–**7**.

Table 1. Data collection parameters for **1**–**7**.

Compound	**1**·py	**2**·HONep, tol	**3**	**4**
Chemical formula	$C_{44}H_{68}N_4O_{12}Ti_3$	$C_{63}H_{106}N_3O_{13}Ti_3$	$C_{45}H_{75}N_3O_{12}Zr_3$	$C_{51}H_{86}N_3O_{12}Zr_3$
Formula weight	988.72	1257.20	1123.74	1206.89
Temp (K)	173 (2)	100 (2)	193 (2)	171 (2)
Space group	Triclinic P −1	Triclinic P −1	Monoclinic P 2_1/c	Monoclinic P 2_1/n
a (Å)	9.5961(16)	15.1701(12)	17.483(2)	14.0736(8)
b (Å)	13.448(2)	15.4643(12)	14.389(2)	25.2166(17)
c (Å)	19.274(3)	17.8934(14)	24.369(3)	21.8384(13)
α (°)	89.262(10)	67.918(3)		
β (°)	86.241(11)	80.384(3)	104.145(2)	105.336(4)
γ (°)	89.834(10)	61.580(2)		
V (Å^3)	2481.7(7)	3420.64	5944.5(14)	7474.2 (8)
Z	2	2	4	4
D_{calcd} (Mg m^{-3})	1.323	1.221	1.256	1.073
μ,(Mo, Kα) (mm^{-1})	0.532	0.401	0.567	0.455
R_1[a] (%) (all data)	8.29 (24.23)	4.70 (5.61)	7.35 (12.65)	9.86 (12.73)
wR_2[b] (%) (all data)	17.11 (26.16)	17.05 (17.96)	18.62 (21.95)	26.16 (24.73)

Compound	**5**	**6**	**7**
Chemical formula	$C_{51}H_{87}Hf_3N_3O_{12}$	$C_{26}H_{44}N_2Nb_2O_{10}$	$C_{44}H_{80}N_2O_{10}Ta_2$
Formula weight	1469.70	730.45	1159.00
Temp (K)	173 (2)	173 (2)	100 (2)
Space group	Monoclinic P 2_1/n	Monoclinic C 2/c	Monoclinic C 2/c
a (Å)	14.0439(5)	18.0874(11)	41.601(2)
b (Å)	25.1417(9)	11.4891(6)	10.5099(4)
c (Å)	21.8499(8)	30.2559(18)	22.3114(10)
β (°)	105.415(2)	91.609(3)	94.048(5)
V (Å^3)	7437.4(5)	6284.9(6)	9730.7(7)
Z	4	8	8
D_{calcd} (Mg m^{-3})	1.313	1.544	1.582
μ,(Mo, Kα) (mm^{-1})	4.221	0.783	4.548
R_1[a] (%) (all data)	6.22 (11.14)	3.26 (4.41)	4.56 (7.38)
wR_2[b] (%) (all data)	17.43 (19.40)	9.29 (11.34)	11.9 (14.34)

[a]$R_1 = \Sigma \mid |F_o| - |F_c| \mid / \Sigma |F_o| \times 100$.
[b]$wR_2 = [\Sigma\, w\,(F_o^2 - F_c^2)^2 / \Sigma\,(w\,|F_o|^2)^2]^{1/2} \times 100$.

Specific issues for problematic structures are presented here: **2** – part instructions were used to model free rotation of the ONep ligands and the free alcohol; **3** – an accessible void of 984.7 Å^3 was squeezed and associated with the loss of three molecules of solvent. In addition, ISOR and EADP were used to model disorder on the *t*-butyl group associated with O(7); **4** – an accessible void of 2694.9 Å^3 was squeezed and associated with the loss of three solvent molecules. ISOR was used on C24 and C25 to model disorder; **5** – EADP used to model disorder on the pendent hydrocarbon chain of the ONep groups.

3. Results and discussion

The number of structurally characterized pdm-modified transition metals is limited to a handful of compounds, including Group 4 (seven compounds – all Ti) or 5 (eight compounds) [1]. For the Group 4 compounds, Fandos and co-workers reported on the

derivatization of pentamethyl-cyclopentadienyl (Cp*) titanium compounds with this ligand [13–16]. In all instances, the pdm modifier acted as a chelate binding through the two O and one N [i.e. η^1,η^1,η^1(O, N, O crystals were used for all additional analyses.), figure 1(d)]. For one complex, (η^5-Cp*)Ti((η^1,η^1,η^1-O,N,O)pdm)(η^1-O)pdm-H)), the second pdm was found in a terminal arrangement with a OH still present. For some of these compounds, the oxygen of pdm was also found to bridge to other metals such as in [(η^5-Cp*)(μ–pdm)Ti(μ_3-O)(Rh(η^2,η^2-cyclooctadiene))$_2$][O_3SCF_3] [14] or [(η^5-Cp*)(μ–pdm)Ti(μ-O)Ir(η^2,η^2-cyclocta-1,5dienyl)] [16]. Several pdm-like ligands with CH_3 [26], C_6H_6 [27], $CH_2C_6H_5$ [28], and cyclo-$C_6H_3(CH_3)$-4$(CH(CH_3)_2)$-1 [25], substituents on the methylene carbons have also been reported. Of these, Rothwell and co-workers formed the α,α-dialkyl-2,6-pyridinemethoxide-N,O,O′ (alkyl = methyl [26] or benzyl [28]) derivative through the carbonylation of a '$M(OAr)_2(CH_3)_2$' precursor; however, this was the result of a chemical transformation and not the direct reaction of the pdm ligand. None of the structurally characterized Group 4 compounds that possess a pdm ligand co-supported by alkoxide ligands are available [1], which prompted a structural study of modified Group 4 metal alkoxides with pdm. For the Group 5 species, the bound ligands can also be divided into pdm [14, 17, 19] and alkyl-substituted pdm (trimethylsilyl prop-2-en-1-olato [29]; -methone [30]) species. Fandos *et al.* also investigated Cp* derivatives of the Group 5 species; in each case, a chelate pdm ligand was reported [14, 17]. This coordination was maintained with bridging when another metal was present as noted by Fites *et al.* for [$NaV(O)_2$ V(μ –pdm)]·$4H_2O$ [19]. Since few structural studies of the early transition metals modified by pdm have been reported [1] and no reports have been disseminated with alkoxide co-ligands, we also chose to explore the structural properties of [$M(OR)_5$] modified by pdm [equation (1); $x = 5$).

3.1. *Synthesis*

Alcoholysis of the various [$M(OR)_4$] with H_2-pdm appeared to proceed cleanly in tol based on the formation of a white precipitate that could be dissolved upon addition of THF/pyridine and/or heat (details in the Experimental section). Slow cooling and evaporation of the volatile component of the reaction mixture led to X-ray quality crystals. The dried powders obtained from these crystals were analyzed by FTIR spectroscopy. The loss of the sharp HO- stretch of H_2-pdm at ~3360 cm^{-1} indicated that the reaction had proceeded as written in equation (1). This is in contrast to several other reports where the pdm-derivatized M^{2+} retained hydroxyl groups [21, 31]. In addition to the stretches and bends of the parent alkoxide ligands, the stretches associated with pdm (1600 and 1577 cm^{-1}) were observed in each spectrum but shifted slightly to higher wave numbers. Little detailed structural understanding was elucidated from the FTIR data and single-crystal structures were obtained when possible to give additional information concerning the coordination behavior of pdm-modified metal alkoxides.

3.2. *Crystal structure*

The 1:1 structure of [$Ti(OPr^i)_4$] with H_2-pdm led to the isolation of an unexpected, trinuclear complex, **1**, which is shown in figure 2. This compound consists of a linearly arranged set of three interlinked '(pdm)$Ti(OPr^i)_2$' moieties with each pdm triply chelating to Ti through the N and both O atoms [chelate mode – figure 1(c)]. Each of the terminal '(pdm)

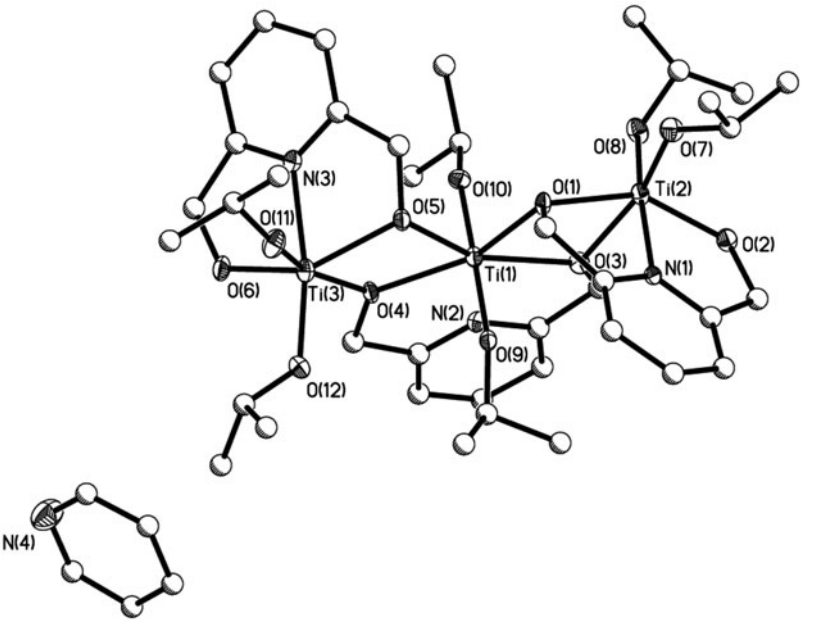

Figure 2. Structure plot of **1** · **py**. Thermal ellipsoids of heavy atoms drawn at the 30% level with carbons drawn as ball and stick and hydrogens omitted for clarity.

$Ti(OPr^i)_2$' fragments also binds to the central Ti through one pdm O forming the μ-pdm [figure 1(d)] geometry. The central fragment uses both of its pdm O atoms [thus μ^3-pdm; figure 1(e)] to bridge back to the terminal moieties. This results in the two terminal Ti ions adopting a distorted *OC*-6 and the central Ti adopting a seven-coordinate geometry. Increasing the steric bulk of the alkoxy ligand to an ONep ligand did not alter the observed final arrangement of **2** (figure 3). Attempts to isolate the Ti-OBu^t-pdm derivative proved fruitless in our hands.

Further studies using a larger cation and its impact on the overall structure was undertaken using the heavier Group 4 congeners. Crystals of $[Zr(OBu^t)_4]$ derivative **3** (figure 4) were solved in a similar construct as noted for **1** and **2**; however, suitable crystals for the Hf-OBu^t derivative were not isolated. Due to the similarity in size and the consistency of the general μ-pdm/μ^3-pdm linear arrangement noted for **1**–**3**, it was anticipated that any Group 4 alkoxide precursor would adopt this structure. Therefore, it was surprising that the Zr-ONep derivative **4** shown in figure 5 had a different arrangement. For this complex, there are three '$(pdm)Zr(ONep)_2$' moieties where each pdm is fully chelated. The Zr(1) and Zr(3) fragments are linked by two μ-ONep ligands. Both of these fragments also use a μ-pdm to bridge to Zr(2). The Zr(2) employs its μ^3-pdm to bridge to both Zr centers to form a ball-shaped molecule. Therefore, the change from the sterically hindering OBu^t to the sterically removed ONep ligand must account for the change in structure. This was confirmed when the Hf-ONep adduct, **5** (figure 6), was also isolated in an identical construct to **4**.

It was of interest to investigate the impact that a higher oxidation state metal would have on the final pdm structures. Therefore, Group 5 species were investigated following equation (1) ($x = 5$) using Nb and Ta alkoxide species. The products isolated were the dinuclear complexes **6** (figure 7) and **7** (figure 8). Compounds **6** and **7** were found to adopt the same

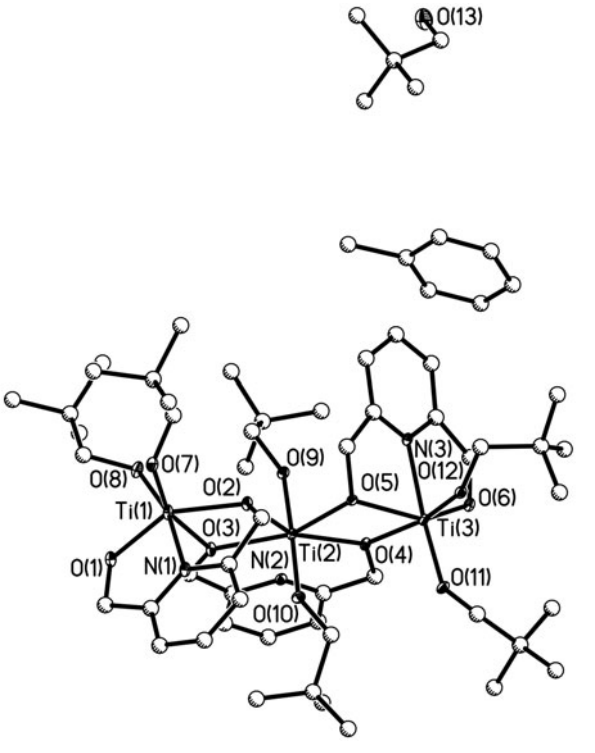

Figure 3. Structure plot of **2** · **HONep, tol**. Thermal ellipsoids of heavy atoms drawn at the 30% level with carbons drawn as ball and stick and hydrogens omitted for clarity.

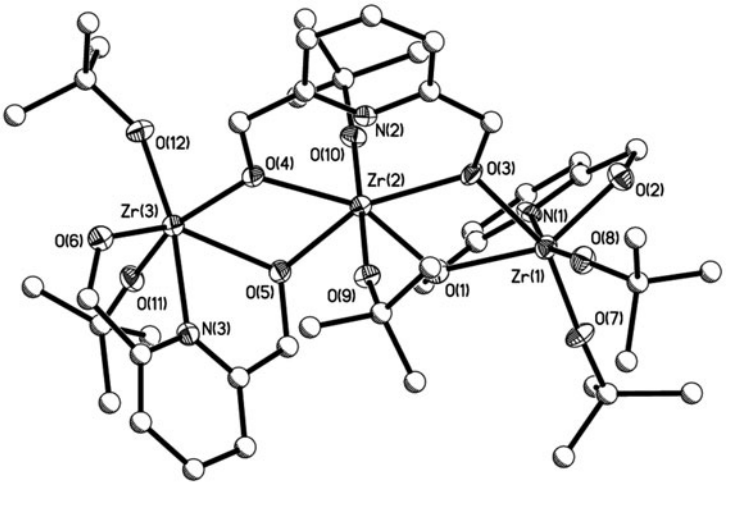

Figure 4. Structure plot of **3**. Thermal ellipsoids of heavy atoms drawn at the 30% level with carbons drawn as ball and stick and hydrogens omitted for clarity.

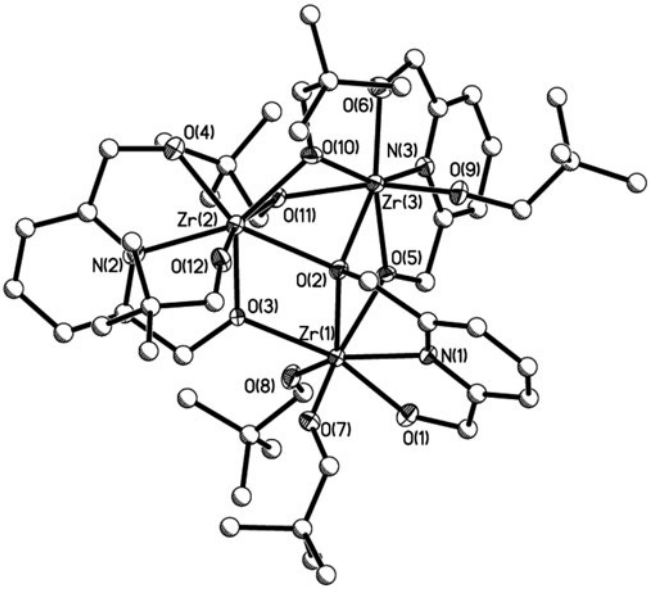

Figure 5. Structure plot of **4**. Thermal ellipsoids of heavy atoms drawn at the 30% level with carbons drawn as ball and stick and hydrogens omitted for clarity.

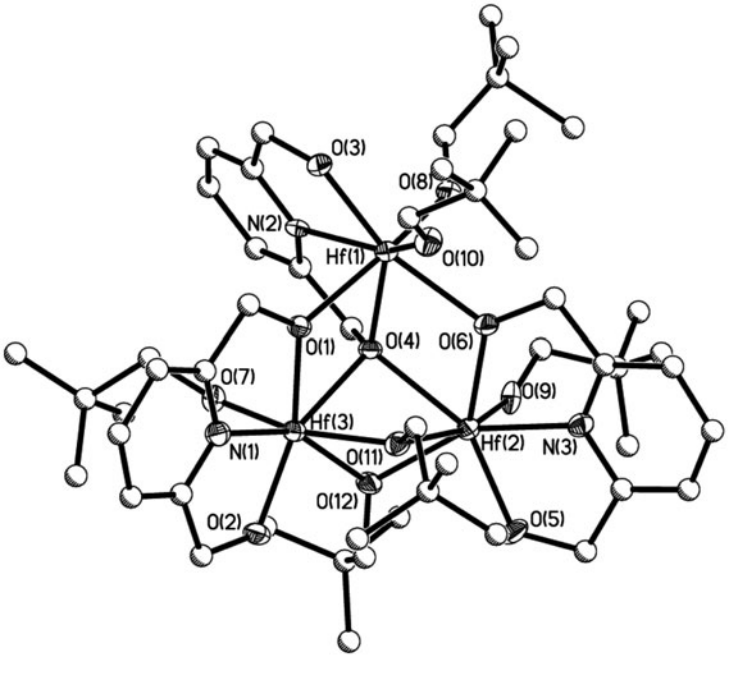

Figure 6. Structure plot of **5**. Thermal ellipsoids of heavy atoms drawn at the 30% level with carbons drawn as ball and stick and hydrogens omitted for clarity. Lattice tol shown.

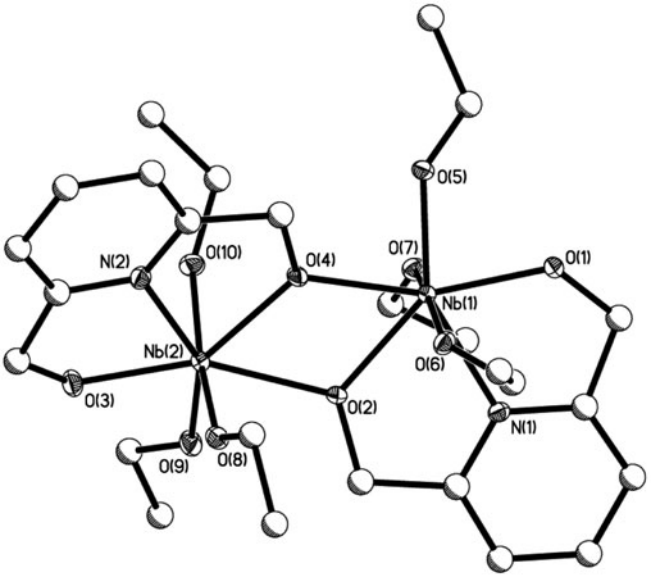

Figure 7. Structure plot of **6**. Thermal ellipsoids of heavy atoms drawn at the 30% level with carbons drawn as ball and stick and hydrogens omitted for clarity.

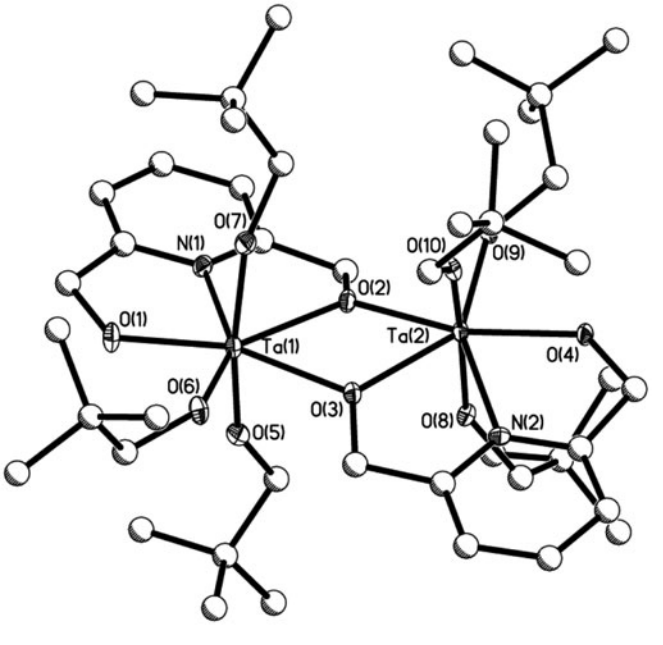

Figure 8. Structure plot of **7**. Thermal ellipsoids of heavy atoms drawn at the 30% level with carbons drawn as ball and stick and hydrogens omitted for clarity.

general construct with a μ-pdm ligand linking the two moieties. Three OR ligands finish off the remaining site to generate a seven-coordinate metal center.

3.3. *Metrical data*

The metrical data for **1**–**7** were compared to each other and reported X-ray structures[1]. In general, when the cation size variation is taken into account, the metrical data (table 2) were in agreement. For the Ti derivatives, [Ti(μ^3-dpm-Ph_2)$_2$] [27] is the best model complex available, as others are carboxylate derivatives or are Cp* derivatives. The distances (Ti–O and Ti–N) and angles for the pdm moieties noted for **1** and **2** are in agreement with those observed for [Ti(μ^3-dpm-Ph_2)$_2$] [27].

For the Zr species, the majority of compounds that possess the general pdm arrangement are again the carboxylate derivatives [1]; however, of those with substitutions on the *alpha* carbon, three are aryloxide derivatives (((η^1,η^1,η^1-O,N,O)pdm-Me)Zr($OC_6H_3(C(CH_3)_3)_2$)(py) and ((η^1,η^1,η^1-O,N,O)pdm-CH_2Ph)Zr($OC_6H_3(C(CH_3)_3)_2$) [26, 28]) and should be reasonable models. The av Zr-O distance of 1.987 Å is in agreement with **4** and **5**; however, the av Zr-N distance of 2.285 Å is significantly shorter than that noted for either **4** or **5**. This variance may be due to the chelating nature of the monomeric literature models forcing a greater interaction in comparison to the bridging trinuclear species of **4** and **5**. A comparison of these compounds does not appear to show any significant deviation in the angles of the pdm moiety around the metal.

For the Hf derivatives, no pdm model is available but the (pyridine-2,6-dicarboylato)hafnium *bis*(η^5-cyclopentadienyl) complex had similar arrangement and was initially used for comparison. The Hf–O distances were much shorter for **6** and **7** *vs*. the model compound (2.176 Å), which was attributed to the electron withdrawing nature of the C=O of the

Table 2. Average metrical data summary for **1**–**7**. Unique values indicated by error bars.

Distances (Å)	M-OR	M-(μ-OR)	M-O_{pdm}	M-(μ_x-O_{pdm}) $x = 2$	M-N_{pdm}	M–M
1	1.84	–	1.89	2.07	2.17	3.36
2	1.85	–	1.89	2.04	2.17	3.39
3	1.95	–	2.02	2.21	2.32	3.60
4	1.96	2.20	2.06	2.21 2.33 ($x = 3$)	2.33	3.58
5	1.97	2.18	2.05	2.20 2.32 ($x = 3$)	2.32	3.56
6	1.93	–	2.00	2.18	2.26	3.642(2)
7	1.92	–	1.99	2.17	2.26	3.662(1)

Angle (°)	RO-M-OR	OR-M-O_{pdm}	O_{pdm}- M-μ-O_{pdm}	μ-O_{pdm}-M-μ_x-O_{pdm} $x = 2$	O_{pdm}-M-N_{pdm}	μ-O_{pdm}-M-N_{pdm}
1	95.9	99.0	143.41	141.45	74.4	71.9
2	93.4	99.8	144.2	143.06	74.7	71.6
3	98.5	98.8	135.0	138.00	70.50	68.5
4	108.10(2)	92.7	136.4	68.0 ($x = 3$)	70.4	68.4
5	106.94(3)	92.9	136.9	68.5 ($x = 3$)	70.9	68.1
6	eq 96.2 ax 167.3	87.5	146.7	64.9	71.4	69.6
7	eq 96.6 ax 166.5	87.6	147.3	64.6	70.9	69.3

carboxylate moiety. Surprisingly, the Hf–N (2.263 Å) distance is in agreement with the model complex, which must be an induced geometrical constraint *vs*. some extended electronic interaction. Compared to other Hf–O distances of 'HfO_3 N' compounds that range from 1.913 to 2.340 Å [1], those noted for **5** fall at the shorter end of this range. The literature Hf–N distances of the 'HfO_3 N' derivatives range from 2.005 to 2.673 Å, in agreement with the values noted for **5**. The angles of **5** are consistent with the literature values.

There are no Nb species that can be used as a model for **6** but two models exist for comparison to **7** [i.e. (Cp*)Ta(O_3SCF_3)$_2$(pdm-C = C-TMS) [32] and [(Cp*)Ta(OH)(pdm)(H_2O)][SO_3CF_3]·H_2O] [17]. Since the cation size is nearly identical for Nb and Ta, these will be used as a model for **6** as well. The av 1.95 Å Ta–O distance is in agreement with **6** and **7**; however, the Ta–N distance was av 2.14 Å and is significantly shorter than that noted for either complex. This may be a reflection of the electron withdrawing nature of the SO_3CF_3 noted for the literature species *vs*. OR ligands used for **6** and **7**.

3.4. *Periodic trends*

The isolation of novel family of compounds allows for some exploration of periodic trends induced by pdm based on cation size and alkoxide variations. Independent of the pendant chain of the alkoxide, the smallest cation Ti (six-coordinate, 0.65 Å) formed the linear chain structure (figures 2 and 3), with a schematic representation shown in figure 9(a). This implies that the structure determination is dominated by the tridentate binding of pdm, preventing any intra-molecular binding. As the larger congeners (six-coordinate: Zr = 0.86 Å, Hf = 0.85 Å) were introduced, it was thought that a more intra-connected species would form. This was not true for **3** (figure 4), which was solved in the linear chain motif, but the intra-connected species [figure 9(b)] were observed for **4** (figure 5) and **5** (figure 6). While both **3** and **4** are Zr adducts, the sterically hindering OBu^t prevents intra-coordination resulting in a linear chain structure. The dislocation of the steric bulk of the ONep moiety allows for a greater interaction between Zr and the various O atoms, forming seven-coordinate Zr (0.92 Å) metal centers in **4**. The impact of the alkoxide steric bulk is further demonstrated by the seven-coordinate Hf (0.90 Å) of **5**, which is smaller than seven-coordinate Zr but larger than the six-coordinate species, yet still yields the same interconnected structure [figure 9(b)]. Therefore, the structural impact of pdm appears countered by the induced steric bulk from the pendant hydrocarbon chain for the larger 4+ congeners.

Investigation of the impact of the charge on the structure obtainable with pdm modified metal alkoxides was undertaken using the Group 5 species. The cations for Nb and Ta are identical in size (six-coordinate 0.78 Å; seven-coordinate 0.83 Å), so it was expected that the resultant structures should be similar. In addition, these cations are intermediate between the smallest Ti cation and the larger congeners Hf and Zr, so either an intra-connected species or a linear chain structure could be observed. As reported previously, **6** and **7** were isolated in the same structural dinuclear arrangement. The increase in charge allows for a more facile accommodation of pdm. Therefore, it appears that the tridentate nature of the pdm has less of a role in determining the final structure in the 5+ species than in the 4+ derivatives.

3.5. *Elemental analyses*

Typically, it is difficult to obtain acceptable elemental analyses of [$M(OR)_x$] due to all the properties that make them of interest for materials production: low thermal decomposition

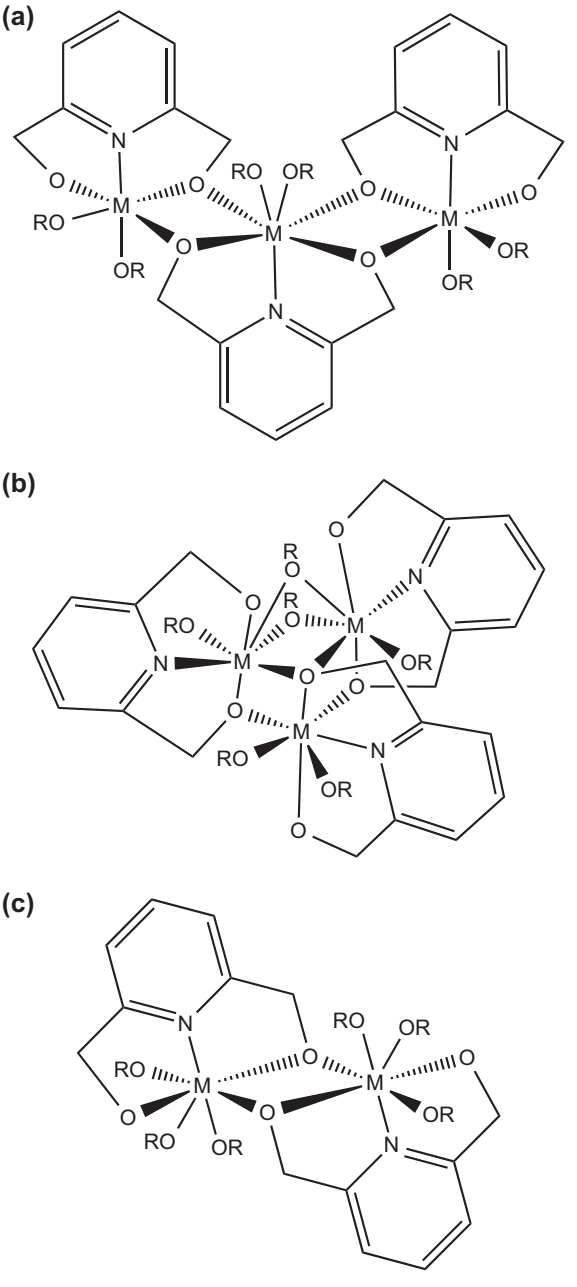

Figure 9. Schematic representation of the isolated structure types: (a) $(OR)_2$ M(μ^2–pdm)[(μ–pdm)M$(OR)_2]_2$ (**1**–**3**), (b) $M_3(\mu^3$–pdm)(μ–pdm$)_2$(ONep$)_6$ (**4**–**5**), and (c) $(OR)_3$ M(μ^2–pdm)$]_2$ (**6** and **7**).

temperatures, tendency to readily hydrolyze/oligomerize, and high volatility. In addition, these compounds are often under-coordinated and bind or trap solvent upon drying. For **1**, **2**, and **6** an acceptable analysis was obtained. For **3** (+py), **4** (+THF), **5** (+py), addition of a crystallization solvent and for **7**, the loss of three methyl groups led to an acceptable

analysis. The addition of solvent and loss of moieties have to be used to account for the analyses of $[M(OR)_x]$ bulk powder [33, 34]. This indicates that the bulk powders are consistent with the crystal structure.

3.6. *Solution state NMR*

It was of interest to determine if the solid-state structure of these compounds were retained in solution. To accomplish this, pulse field gradient-diffusion ordered spectroscopy (PFG/DOSY) experiments were considered a viable means to determine the solution state structure. This experiment works by identifying the different chemical species present in solution based on their diffusion coefficient, which can be interpreted relating to the size or shape of the molecule. From these data (see table 3), it was determined that only a single component was present in solution since the final ratio recorded $\neq$ 1. Unfortunately, the other data do not assist in identifying the structure of the complex in solution. However, standard ^{1}H NMR data did lend some insight into the solution behavior of these compounds.

The ^{1}H NMR spectrum of the H_2-pdm shows the expected triplet (7.64 ppm), doublet (7.13 ppm), and singlet (4.72 ppm) for the *para*, *ortho*, and methylene protons, respectively, along with a broad singlet at δ 3.23 for the OH peak. The –OH peak is absent in each of the subsequent ^{1}H NMR spectra of **1**–**7**. The ^{1}H and ^{13}C NMR spectra of **1**–**7** were collected in a variety of solvents (py-d_5, THF-d_8, acetone-d_6, $CDCl_3$) in an attempt to get interpretable spectra. The spectra collected of the samples dissolved in $CDCl_3$ yielded useful information and are discussed below. It is of note for these spectra, an extended relaxation time was applied to the samples in order to achieve stable and meaningful integration results.

For the ^{1}H NMR spectra of the like structured **1**–**3**, two sets of ligand types (i.e. pdm and OR) were expected for the terminal and bridging ligands, with a 2:1 ratio if the compound remained stable in solution. For **1**–**3**, the expected pdm resonances were observed with the methylene resonances in a roughly 2:1 ratio. The methine septuplets of **1** and broad singlets for the methylene of **2** were also noted in a 2:1 ratio. The methyl resonances of **1**–**3** were multiple and overlapping. Combining these spectra indicate that the solid-state structures of **1**–**3** were retained in solution.

The spectra of **4**–**5** involve complex solid-state structures that have numerous inequivalent ligand species present. When this is coupled with the expected diastereotopic methylene, phenyl rings, and alkoxides, the spectra were calculated to be very complex. In addition, the low solubility of these compounds was expected to further complicate interpretation of the NMR data. While the pdm resonances and alkoxide

Table 3. PFG/DOSY data for **2**–**6**.

Name	D (m^2 s^{-1})/e-10	Å	Å^3	Ratio
Pyridine	17	1.43541	12.3884	1
2	6.1	4.05159	278.59	22.488
3	7.5	3.29926	150.432	14.143
4	2.7	9.08566	3141.65	253.597
5	6.1	4.08967	286.519	23.128
6	9.4	2.62753	75.9854	6.1336

resonances could be identified for **4**–**5**, the overlapping, complex set of resonances observed made interpretation tentative. Therefore, these are not listed in the experimental section, as no meaningful solution understanding could be presented; however, it is of note that clusters of resonances observed were in agreement with the expected peaks for the various OR and pdm ligands.

The dinuclear structures of **6** and **7** were expected to yield one set of pdm resonances and two types of OR resonances. For **6**, the spectrum described above was observed. If the monomer was present, then the OEt groups would be equivalent and only one set of resonances should be present; however, the 1:2 ratio noted for both the methylene and methyl resonances argues for a dinuclear complex. For **7**, the larger ONep ligands may play a role in stabilizing a monomeric species. However, there are numerous pdm methylene and methyl resonances observed. Therefore, definitive conclusions of the nuclearity in solution of this complex could not be made.

4. Summary and conclusion

A new family of pdm-modified metal alkoxide complexes has been isolated (**1**–**7**). For each instance, the pdm ligand is bound in a tridentate manner; however, for all of the compounds, at least one of the pdm-O atoms bridges to another metal. For the group 4 species, this resulted in either a linear structure $(OR)_2M(\mu^2\text{–pdm})[(\mu\text{–pdm})M(OR)_2]_2$ (**1**–**3**) or a more interconnected complex $M_3(\mu^3\text{–pdm})(\mu\text{–pdm})_2(ONep)_6$ (**4**–**5**). The Group 5 species adopted simple dinuclear complexes (**6** and **7**). The solution state was difficult to discern but the NMR data appear to support retention of the structure in solution. The variations noted in the tridentate pdm-modified structure types isolated were further impacted by the size of the cation, the steric bulk of the pendant chain of the alkoxide used, and the charge of the metal cation. By systematically varying these characteristics, it is reasoned that we will be able to tune the structure types available for pdm-modified metal alkoxides. This is being investigated by altering the alkyl moiety and the metals in conjunction with the pdm ligand.

Supplementary material

CCDC 1041173-1041179 contains the supplementary crystallographic data for **1**–**7**, respectively. These data can be obtained free of charge via http://www.ccdc.cam.ac.uk/conts/retrieving.html, or from the Cambridge Crystallographic Data Center, 12 Union Road, Cambridge CB2 1EZ, UK; fax: (+44) 1223–336-033; or E-mail: deposit@ccdc.cam.ac.uk.

Acknowledgments

This work was supported by the Laboratory Directed Research and Development (LDRD) programs at Sandia National Laboratories and the National Science Foundation CRIF:MU award to Prof Kemp of the University of New Mexico (CHE04-43580) for purchase of a Bruker X-ray diffractometer. Sandia National Laboratories is a multi-program laboratory managed and operated by Sandia Corporation, a wholly owned subsidiary of Lockheed

Martin Corporation, for the US Department of Energy's National Nuclear Security Administration under contract DE-AC04-94AL85000.

Disclosure statement

No potential conflict of interest was reported by the authors.

References

[1] Conquest Version 1.14. Cambridge Crystallographic Data Centre. Available online at: support@ccdc.cam.ac.uk or http://www.ccdc.cam.ac.uk [CSD version 5.35 (accessed November 2013)].
[2] D.C. Bradley, R.C. Mehrotra, I.P. Rothwell, A. Singh. *Alkoxo and Aryloxo Derivatives of Metals*, Academic Press, San Diego, CA (2001).
[3] K.G. Caulton, L.G. Hubert-Pfalzgraf. *Chem. Rev.*, **90**, 969 (1990).
[4] U. Schubert, U. Bauer, H. Fric, M. Puchberger, W. Rupp, V. Toma. In *Organic/Inorganic Hybrid Materials-2004*, C. Sanchez, U. Schubert, R.M. Laine, Y. Chujo (Eds.), pp. 533–538, Materials Research Society, Boston, MA (2005).
[5] P.L. Diaconescu. *Comments Inorg. Chem.*, **31**, 196 (2010).
[6] M. Napoli, C. Saturnino, E.I. Cianciulli, M. Varcamonti, A. Zanfardino, G. Tommonaro, P. Longo. *J. Organometallic Chem.*, **725**, 46 (2013).
[7] C.-Y. Li, C.-J. Yu, B.-T. Ko. *Organometallics*, **32**, 172 (2013).
[8] Z.H. Zhou, H.X. Wang, P. Yu, M.M. Olmstead, S.P. Cramer. *J. Inorg. Biochem.*, **118**, 100 (2013).
[9] G. Torres, Y. Ishikawa, J.A. Prieto. *J. Phys. Org. Chem.*, **25**, 1299 (2012).
[10] A. Bartoszewicz, R. Marcos, S. Sahoo, A.K. Inge, X.D. Zou, B. Martín-Matute, *Chem. Eur. J.*, **18**, 14510 (2012).
[11] T.J. Boyle, R.M. Sewell, L.A.M. Ottley, H.D. Pratt, C.J. Quintana, S.D. Bunge. *Inorg. Chem.*, **46**, 1825 (2007).
[12] T.J. Boyle, L.A.M. Ottley, M.A. Rodriguez, R.M. Sewell, T.M. Alam, S.K. McIntyre. *Inorg. Chem.*, **47**, 10708 (2008).
[13] R. Fandos, B. Gallego, A. Otero, A. Rodríguez, M.J. Ruiz, P. Terreros, C. Pastor. *Organometallics*, **26**, 2896 (2007).
[14] R. Fandos, A. Otero, A. Rodríguez, M.J. Ruiz, P. Terreros. *J. Organometallic Chem.*, **689**, 2641 (2004).
[15] R. Fandos, B. Gallego, M.I. López-Solera, A. Otero, A. Rodríguez, M.J. Ruiz, P. Terreros, T. van Mourik. *Organometallics*, **28**, 1329 (2009).
[16] R. Fandos, C. Hernández, A. Otero, A. Rodríguez, M.J. Ruiz, P. Terreros. *Chem. Eur. J.*, **9**, 671 (2003).
[17] A. Conde, R. Fandos, A. Otero, A. Rodríguez. *Organometallics*, **26**, 1568 (2007).
[18] R. Fandos, I. López-Solera, A. Otero, A. Rodríguez, M.J. Ruiz, P. Terreros. *Organometallics*, **23**, 5030 (2004).
[19] R.J. Fites, A.T. Yeager, T.L. Sarvela, W.A. Howard, G. Zhu, K. Pang. *Inorg. Chim. Acta*, **359**, 248 (2006).
[20] J.M. Berg, R.H. Holm. *Inorg. Chem.*, **22**, 1768 (1983).
[21] M. Murugesu, A. Mishra, W. Wernsdorfer, K.A. Abboud, G. Christou. *Polyhedron*, **25**, 613 (2006).
[22] T.J. Boyle, T.M. Alam, E.R. Mechenbier, B.L. Scott, J.W. Ziller. *Inorg. Chem.*, **36**, 3293 (1997).
[23] T.J. Boyle, L.A.M. Ottley, S.M. Hoppe. *Inorg. Chem.*, **49**, 10798 (2010).
[24] T.J. Boyle, J.J. Gallegos, D.M. Pedrotty, E.R. Mechenbier, B.L. Scott. *J. Coord. Chem.*, **47**, 155 (1999).
[25] P.E. Fanwick, L.M. Kobriger, A.K. McMullen, I.P. Rothwell. *J. Am. Chem. Soc.*, **108**, 8095 (1986).
[26] K.V. Zaitsev, M.V. Bermeshev, S.S. Karlov, Y.F. Oprunenko, A.V. Churakov, J.A.K. Howard, G.S. Zaitseva. *Inorg. Chim. Acta*, **360**, 2507 (2007).
[27] C.H. Zambrano, A.K. McMullen, L.M. Kobriger, P.E. Fanwick, I.P. Rothwell. *J. Am. Chem. Soc.*, **112**, 6565 (1990).
[28] R.M. Gauvin, J.A. Osborn, J. Kress. *Organometallics*, **19**, 2944 (2000).
[29] A. Conde, R. Fandos, C. Hernández, A. Otero, A.M. Rodríguez, M.J. Ruiz. *Chem. Eur. J.*, **18**, 2319 (2012).
[30] S. Belemin-Laponnaz, K.S. Coleman, P. Dierkes, J.-P. Masson, J.A. Osborn. *Eur. J. Inorg. Chem.*, 1645 (2000).
[31] R. Fandos, B. Gallego, M.I. López-Solera, A. Otero, Ana Rodríguez, María José Ruiz, Pilar Terreros. *Organometallics*, **28**, 1329 (2009).
[32] A. Conde, R. Fandos, C. Hernández, A. Otero, A. Rodríguez, M.J. Ruiz. *Chem. Eur. J.*, **18**, 2319 (2012).
[33] T.J. Boyle, L.A. Steele, P.D. Burton, S. Hoppe, C. Lockhart, M.A. Rodriguez. *Inorg. Chem.*, **51**, 12075 (2012).
[34] T.J. Boyle, D.T. Yonemoto, T.Q. Doan, T.M. Alam. *Inorg. Chem.*, **53**, 12449 (2014).